EXPERIMENTAL STUDY OF THE FLOW PAST A CUBE WITH OPENINGS EMBEDDED IN A TURBULENT BOUNDARY LAYER

Marinos Manolesos

State Key Laboratory of Atmospheric Boundary Layer Physics and Atmospheric Chemistry,
Institute of Atmospheric Physics, Chinese Academy of Sciences
Beijing 100029, China
Email: marinos@fluid.mech.ntua.gr

Zhiqiu Gao

State Key Laboratory of Atmospheric Boundary Layer
Physics and Atmospheric Chemistry,
Institute of Atmospheric Physics,
Chinese Academy of Sciences
Beijing 100029, China
Email: zgao@mail.iap.ac.cn

Zhou Xing

China-EU Institute for Clean & Renewable Energy
Huazhong University of Science and Technology
1037 Lyuoyu Rd., 430074, Wuhan, China

Meletis Panos

School of Mechanical Engineering
National Technical University of Athens
9 Heroon Polytechnioy, 15780 Zografou, Greece
Email: meletpan@yahoo.gr

Demetri Bouris

School of Mechanical Engineering
National Technical University of Athens
9 Heroon Polytechniou, 15780 Zografou, Greece
Email: dbouris@fluid.mech.ntua.gr

ABSTRACT

The present study deals with the effect of inflow shear and ventilation openings on the flow around a surface mounted cube embedded in a turbulent boundary layer. In total, 8 different combinations of upstream boundary layer, cube orientation and openings distribution on the cube sides are examined for a Reynolds number of 24000, based on the cube side and free stream velocity at the cube height. The effect of the shear is significant, altering the mean flow patterns both above and downstream of the cube. Higher inflow shear leads to earlier reattachment, and modified flow patterns in the wake. The openings appear to also significantly alter the flow topology in the vicinity of the cube, with a less pronounced effect on the pressure distribution.

INTRODUCTION

The configuration of a surface mounted prism exposed to a turbulent boundary layer has been the subject of numerous experimental studies in the past (Castro and Robins 1977, Kawai and Nishimura, 1996; Kawai, 2002; Marwood and Wood, 1997; Tieleman and Akins, 1996; Tieleman et al, 2003). Most of these investigations, however, dealt with the unsteady aerodynamics forces that are experienced by the prism, particularly the roof. Focus was therefore placed on the mechanisms responsible for instances of extreme forces and how these are related to the upstream boundary layer characteristics such as turbulence intensity, length scale and profile shape.

It has been documented (Costola et al., 2010) that the surface pressure distribution is an important parameter when calculating ventilation and infiltration rates and consequently issues of air quality in and around the building. However, there is only a limited number of studies dealing with the of effect of the upstream boundary layer characteristics on the surface pressure distribution, especially when there are openings on the surfaces of the prism (Van Moeseke et al., 2005; Syrios and Hunt, 2008).

In the present study, the case of a surface mounted cube at two different orientations (0° and 45°) exposed to an upstream turbulent boundary layer is examined. The effects of the boundary layer's turbulence characteristics as well as the presence of openings on its vertical faces are investigated.

EXPERIMENTAL SET UP
Wind tunnel and cube model

All experiments were performed in the large (3.5m x 2.5m x 12.0m – width x height x length) test section of the National Technical University of Athens wind tunnel. The building model (**Figure 1**) was a cube of 0.11m height made from 5mm thick plexiglass sheets with slot openings of 90x6 mm^2 on each vertical side. The openings correspond to 4.5% of each side area and may be fully or partially covered, depending on the desired opening orientation and distribution. 42 pressure taps were fitted to one of the vertical sides and another 49 to the roof of the cube. The tubing was concealed using a second layer of plexiglass and a 22x22 mm hollow column in the centre of the cube in order to clearly define the inner geometry of the cube. Measurements of surface pressures on all sides of the cube with respect to the flow were performed by rotating the turntable, at the centre of which the cube was mounted.

Two different upstream boundary layers were examined using a combination of spires and roughness elements (Irwin, 1981) in

order to vary mean velocity profiles, surface shear stress, turbulence intensity and length scales.

Two different opening configurations were examined in order to investigate the effects on the pressure distribution and on the flow in and around the cube. One configuration had all the openings closed, while the other had two openings open, namely those at the upstream and downstream side of the cube. Each configuration was measured at 0° and 45° incidence and for both boundary layer profiles.

Table 1 lists the cases examined in this study. For simplicity, the two configurations are referred to as Closed and Open in the following paragraphs, while the two different inflow profiles are named based on their mean velocity shear characteristic, although naturally more parameters change at the same time.
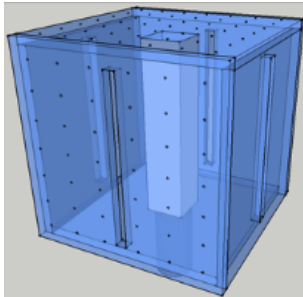
Figure 1. Plexiglass cube with visible slot openings, pressure tap positions and the inner column concealing the pressure tubing.

Measurement set up

Surface pressure measurements were performed using a pressure scanner (FCS421, Furness Controls Ltd) and a differential manometer (FCO16, Furness Controls Ltd), while a TSI Inc. IFA 300 measurement system was used for the hot wire measurements in the cube wake.

Two 4Mpixel cameras and TSI Inc. equipment and software were used for the Stereo Particle Image Velocimetry (PIV) tests. The cameras were located at the sides of the model and the laser sheet was directed to the desired location by means of a mirror located on the wind tunnel traverse system, well above the cube.

Measurements were taken at 7 planes for both orientations, as shown schematically in Figure 2 to Figure 5. At each plane, measurements were taken for all four cases given in Table 1. Two additional planes were measured for the rotated cases, as shown in Figure 5. For each plane, 1000 snapshots were taken and the results presented here are the averaged data.

Figure 2. Side view of the measurement planes for the 0° orientation. The flow is from right to left and the cube is dark blue.
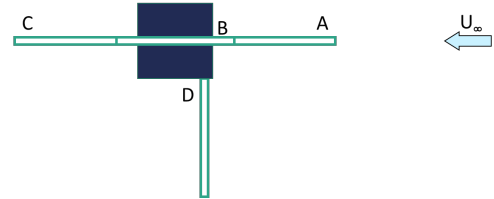
Figure 3. Top view of the measurement planes for the 0° orientation. The flow is from right to left and the cube is dark blue.
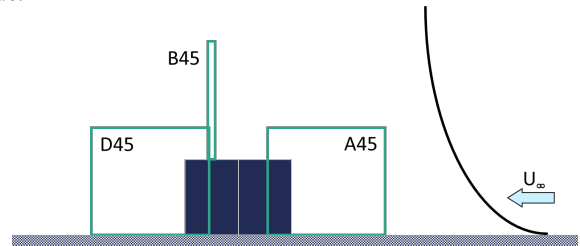
Figure 4. Side view of the measurement planes for the 45° orientation. The flow is from right to left and the cube is dark blue.
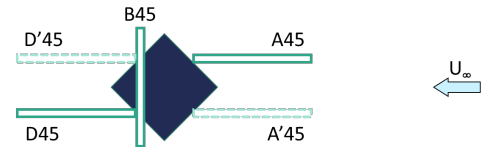
Figure 5. Top view of the measurement planes for the 45° orientation. The flow is from right to left and the cube is dark blue. Dashed lines indicate additional measurement planes (A'45, D'45) for the Open configuration.

A pulse separation time of 85 μsec was used as higher values would increase the measurement noise and make peak detection harder. The corresponding minimum resolved velocity (the

Table 1. The cases examined in the present study

Case	Inflow	Openings	Incidence
1	High Shear	Closed	0°
2	High Shear	Open	0°
3	Low Shear	Closed	0°
4	Low Shear	Open	0°
5	High Shear	Closed	45°
6	High Shear	Open	45°
7	Low Shear	Closed	45°
8	Low Shear	Open	45°

Table 2. Stereo PIV measurement planes

Plane	Cube angle	Plane orientation wrt the free stream	Cases
A	0°	Parallel	All
B	0°	Parallel	All
C	0°	Parallel	All
D	0°	Normal	All
A45	45°	Parallel	All
B45	45°	Normal	All
D45	45°	Parallel	All

| A'45 | 45° | Parallel | 5 – 8 |
| D'45 | 45° | Parallel | 5 – 8 |

velocity corresponding to displacement of 0.1px, Foucaut et al. 2004; Westerweel , 2000]) was equal to 0.12m/s, any values below this should not be trusted.

For all planes the number of spurious vectors was always below 5% and spurious vectors were replaced using a 3×3 vector local mean. The particle displacement was in all cases less than 1/4 of the 32×32px interrogation area and a 50% overlapping was used, which lead to a spacing of 1.8mm between vectors in all dimensions.

RESULTS
Simulated Atmospheric Boundary Layer

The measured boundary layer profiles had the same mean velocity at the cube height, but different turbulence intensity and mean velocity shear profiles (Figure 6). The resulting aerodynamic roughness length and friction velocity were: z_o=2.6 mm, $u*$=0.37 m/s for the High Shear profile and z_o=0.12 mm, $u*$=0.2 m/s for the Low Shear one. The velocity at the cube height was U_H=3.4 m/s, which corresponds to a Reynolds number of 24000, well over the suggested limit for Reynolds number independence of the flow (Castro and Robins, 1977, Lim et al., 2007). The velocity well above the simulated boundary layer was $U_\infty \approx 5.1$ m/s for both cases.

The spectra of the measured velocity field at cube height is given in Figure 7, where it can be seen that it follows a -5/3 inertial subrange slope for more than a decade of non-dimensional frequency.

Turbulence intensity in the free stream, well above the cube was <2%, increasing towards the floor due to the combined effects of the spires and the surface roughness elements. Based on the boundary layer mean profile and turbulence characteristics, we calculated the model scale factor according to Cook (1978) and found it relatively invariable at 1:400, up to a height of ~0.3m i.e. 3 times the model height.

Flow around the cube

Given the limited length of the present paper and the relatively large amount of data, only selected results are presented herein. Contours of streamwise velocity and measured Reynolds stresses for the case where the cube was normal to the flow are given in Figure 8 to Figure 11. Measurements from the rotated cube test cases are given in Figure 12 and Figure 13. The cube height and the freestream velocity measured at a location well above the incoming boundary layer are used as a reference values to non-dimensionalise the results.

From the results concerning cases 1-4, i.e. where the cube was located normal to the flow, it is found that the flow topology along the cube centreline depends strongly on the incoming flow shear profile. Reattachment occurs earlier for the high shear cases and a saddle point appears on the flow lines in the wake of the cube model. Pressure measurements also confirm that the flow reattaches earlier in the high shear cases, as shown in Figure 14.

It is conceivable that as the high shear profile contains lower total momentum up to the cube height, the upwash close to the cube will be weaker and hence the recirculation region smaller. Similarly, the flow in the wake is not as curved towards the floor

and the saddle point appears in the wake. On the contrary, the low shear profile contains more momentum, which is first diverted
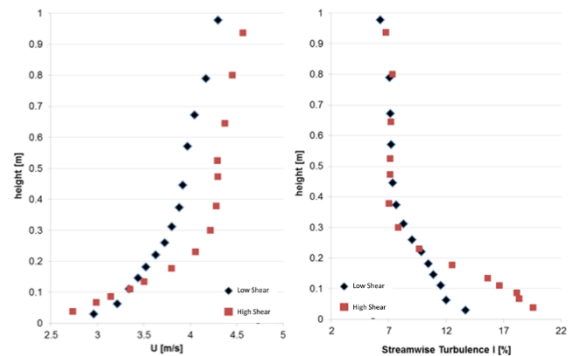
Figure 6. Measured profiles of mean velocity (left) and streamwise turbulence intensity (right) corresponding to the Low and High Shear inflow cases.
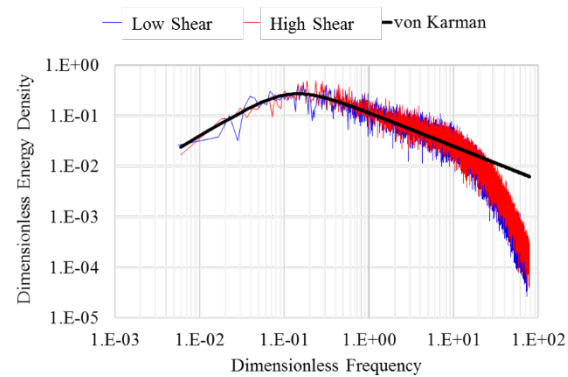
Figure 7. Non-dimensional spectra of the velocity at cube height.

upwards, upstream of the cube, creates a larger recirculation zone above it and then flows downwards in the cube wake. The above explanation is in agreement with Hearst et al., 2016, who found that the mean flow around the cube is dominated by the inflow shear and velocity at cube height rather than the turbulence intensity of the incoming profile.

The effect of the relatively small openings is seen both on the in-plane flow lines (Figure 8) as well as on the normal Reynolds stresses contours (Figure 9 and Figure 10). The mean flow appears to come out of the openings in the wake and joins the wake vortex, which is moved downstream. Streamwise velocity fluctuations are increased in the vicinity of the downstream opening. At the same time v' (Figure 11) and w' (not shown here) velocity fluctuations decrease further downstream, as a result of the openings presence. The effect of the opening is similar for the two inflow cases, also in agreement with the pressure measurements (not shown here for brevity).

For the rotated cube cases, it is found that the Low Shear inflow leads to stronger conical vortices, probably through the same mechanism of intense upwash due to the increased momentum of the profile that was outlined earlier. On the other hand, openings lead to weaker vortices with a small asymmetry between the two. In all cases, the combined downwash of the roof conical vortices brings high velocity fluid from the freestream

towards the cube, while both vortices turn lower velocity fluid away from the cube at the sides (Figure 12).
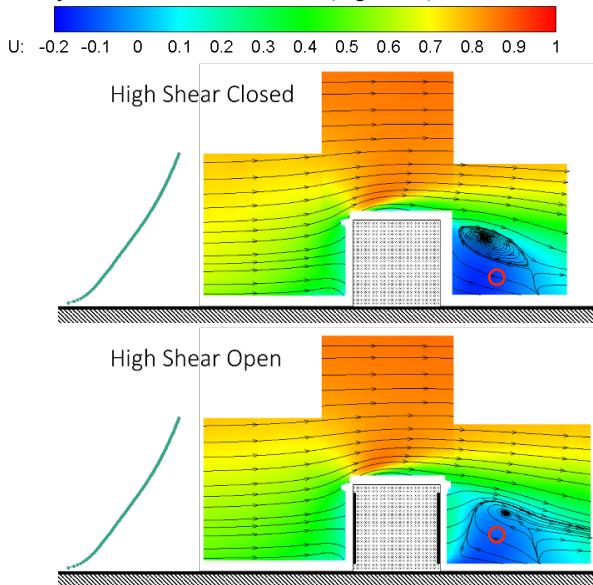
Figure 8. Free stream velocity contours on the planes along the cube centreline (A, B and C) for the High Shear cases at 0° (cases 1 and 2). Saddle point location indicated by a red circle.
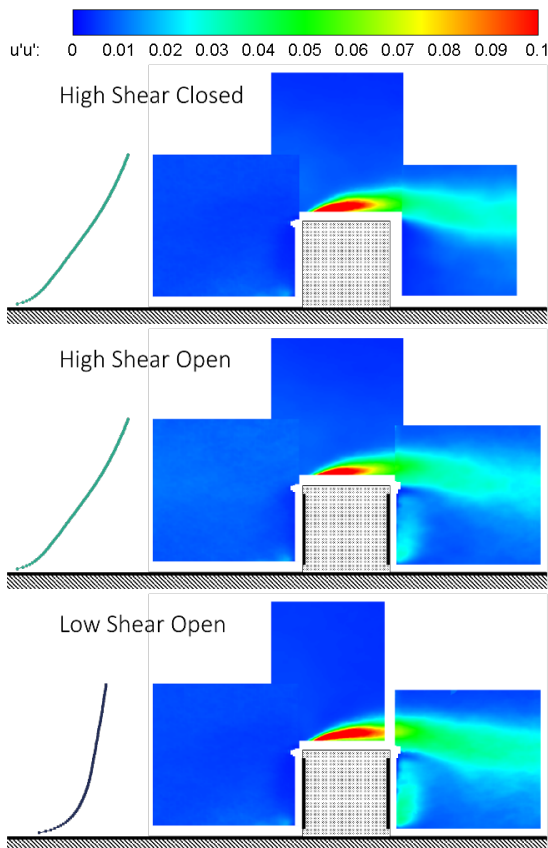
Figure 9. Normalized $u'u'$ normal Reynolds stress contours on the planes along the cube centreline (A, B and C) for the High Shear cases (cases 1 and 2) and for the Low Shear Open case (4) at 0°.
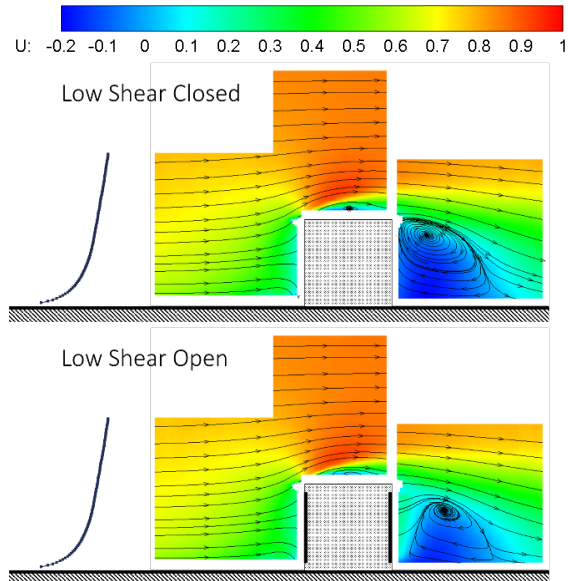
Figure 10. Free stream velocity contours on the planes along the cube centreline (A, B and C) for the Low Shear cases at 0° (cases 3 and 4). No saddle point observed in the wake.
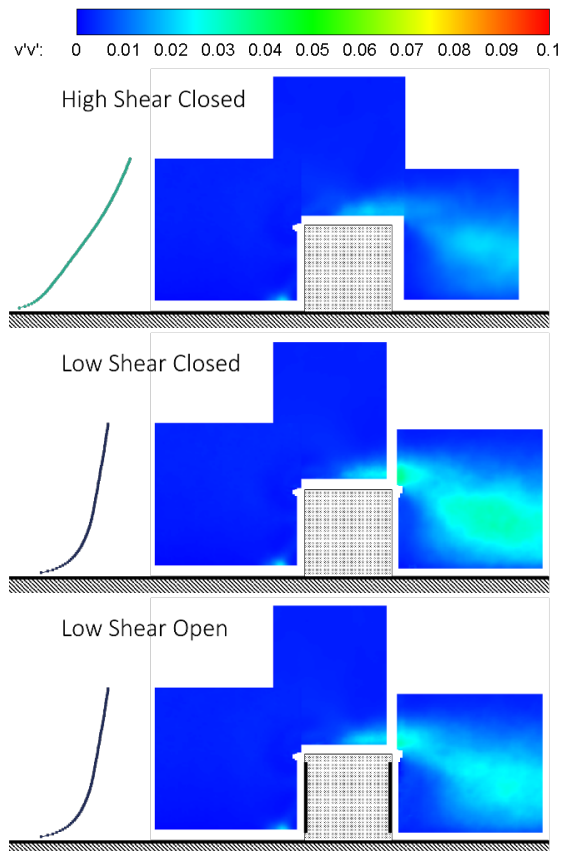
Figure 11. Normalized $v'v'$ normal Reynolds stress contours on the planes along the cube centreline (A, B and C) for the High Shear Closed case (1) and for the Low Shear cases (cases 3 and 4) at 0°.
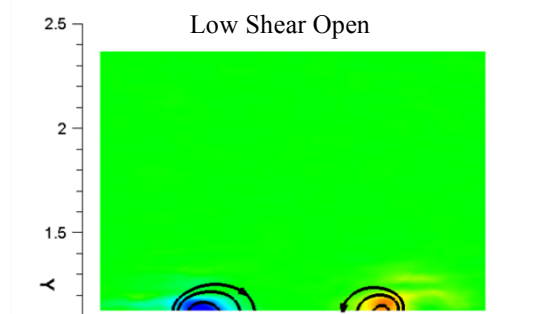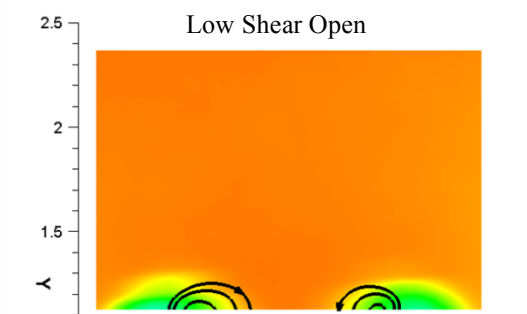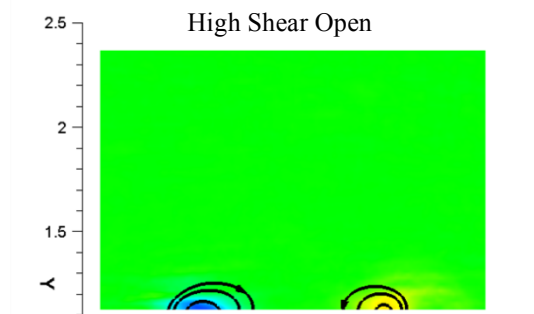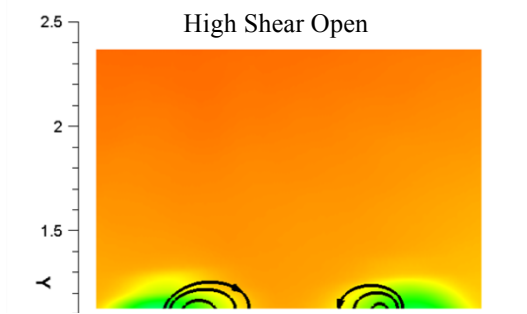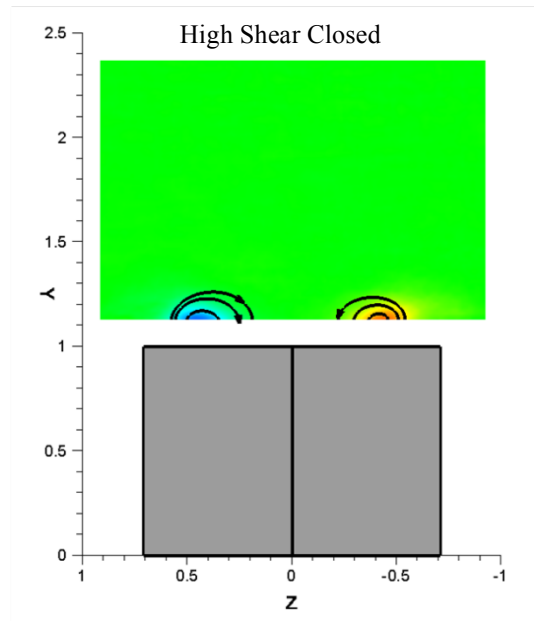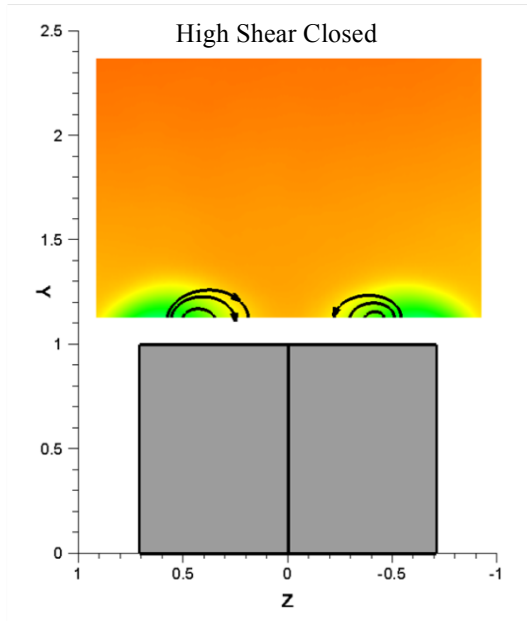
Figure 12. Streamwise velocity contours on the plane above the cube (B45) for the High Shear cases (cases 5 and 6) and for the Low Shear Open case (8) at 45°. The view is from downstream and the cube is only shown in the top figure.

Figure 13. Normalized vorticity contours on the plane above the cube (B45) for the High Shear cases (cases 5 and 6) and for the Low Shear Open case (8) at 45°. The view is from downstream and the cube is only shown in the top figure.

Combining the Stereo PIV and pressure measurements for the low shear cases, it is found that although the mean and turbulence characteristics of the flow are significantly altered by the presence of the openings, the pressure on the lee side of the cube does not appear to be significantly affected (Figure 14, bottom). This indicates that the openings investigated in the present study are not

expected to significantly alter the pressure loads on a building. However, they could have a measurable effect on the flow around it, affecting thus pedestrian comfort. Further research is required to determine possible effects on infiltration and ventilation, which depend on differential pressure across the envelope.

5
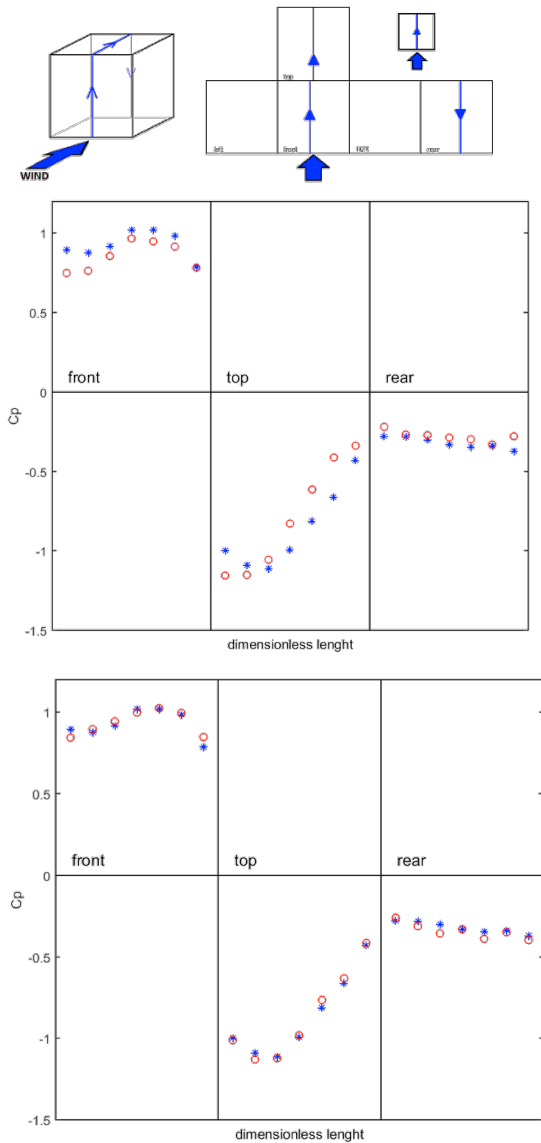
Figure 14. Pressure coefficient distribution along the cube centreline (path shown at top) for cases 1 and 3 (middle) and 3 and 4 (bottom).

CONCLUSIONS

The flow around a surface mounted cube exposed to a turbulent boundary layer is experimentally studied using wind tunnel simulations. Two different cube orientations are examined in relation to the upstream turbulent boundary layer and the presence of openings on the cube.

Pressure taps on the cube surface allowed measurements of pressure distributions, hot wire anemometry is used for characterising the velocity frequency spectrum and stereoscopic particle image velocimetry is planned in order to provide overall insight of the flow structure.

Results show that both the inflow shear and the opening have a significant effect on the flow around the cube. Given the limited extend of the present paper only a limited number of findings is presented including the effect of inflow shear on mean flow

reattachment length, and the effect of the openings and shear on flow topology. Interestingly, cases were observed where the mean flow was altered significantly by the presence of the openings with only subtle changes to the pressure distribution on the cube surface.

REFERENCES

Castro I. and Robins A., 1977, "The flow around a surface mounted cube in uniform an turbulent streams". J. Fluid Mech., Vol. 79, No. 2, pp. 307-335.

Cook N J. 1978, "Determination of the model scale factor in wind-tunnel simulations of the adiabatic atmospheric boundary layer". Journal of Wind Engineering and Industrial Aerodynamics, Vol 2(4), pp 311-321.

Cóstola, D.; Blocken, B.; Ohba, M.; Hensen, J.L.M. Uncertainty in airflow rate calculations due to the use of surface-averaged pressure coefficients. Energy Build 2010, 42, 881–888.

Foucaut J. M., Miliat B., Perenne N., and Stanislas M., "Characterization of different PIV algorithms using the EUROPIV synthetic image generator and real images from a turbulent boundary layer," in Particle Image Velocimetry: Recent Improvements, Springer, 2004, pp. 163–185.

Hearst RJ, Gomit G, Ganapathisubramani B. Effect of turbulence on the wake of a wall-mounted cube. Journal of Fluid Mechanics. 2016 Oct;804:513-30.

Irwin, H. (1981). The design of spires for wind simulation. Journal of Wind Engineering and Industrial Aerodynamics, 7(3), 361-366.

Kawai H, Nishimura G., 1996, "Characteristics of fluctuating suction and conical vortices on a flat roof in oblique flow". J. Wind Eng. Ind. Aerodyn. Vol 60, pp. 211-225.

Kawai H., 2002, "Local peak pressure and conical vortex on building." J. Wind Eng. Ind. Aerodyn., Vol 90, pp. 251-263.

Lim, Hee Chang, Castro I. P., and Hoxey R. P., 2007. "Bluff bodies in deep turbulent boundary layers: Reynolds-number issues." J. Wind Eng. Ind. Aerodyn. Vol 571 pp. 97-118.

Marwood R. and Wood C.J., 1997, "Conical vortex movement and its effect on roof pressures" J. Wind Eng. Ind. Aerodyn., Vol. 69-71, pp. 589-595.

Syrios K., Hunt G.R., Passive air exchanges between building and urban canyon via openings in a single façade. Int. J. Heat Fluid Flow 2008, 29, 364–373

Tieleman H., Ge Z., Hajj M., Reinhold T., 2003, "Pressures on a surface-mounted rectangular prism under varying incident turbulence", J. Wind engineering and Industrial Aerodynamics, Vol. 91, pp. 1095-1115.

Tieleman, H. and Akins, R., 1996, "The effect of Incident Turbulence on the Surface Pressures of Surface Mounted Prisms", J. Fluids and Structures, Vol. 10, 367-393.

Van Moeseke G., Gratia E., Reiter S., De Herde A. Wind pressure distribution influence on natural ventilation for different incidences and environment densities. Energy Build 2005, 37, 878–889.

Westerweel J., "Theoretical analysis of the measurement precision in particle image velocimetry," Exp. Fluids, vol. 29, no. 1, pp. S003–S012, 2000.